World Academy of Science, Engineering and Technology
International Journal of Mechanical and Mechatronics Engineering
Vol:9, No:5, 2015

Experimental and Numerical Analysis of Built-In Thermoelectric Generator Modules with an Elliptical Pin-Fin Heat Sink

J. Y Jang, C. Y. Tseng

***Abstract*—**A three-dimensional numerical model of thermoelectric generator (TEG) modules attached to a large chimney plate is proposed and solved numerically using a control volume based finite difference formulation. The TEG module consists of a thermoelectric generator, an elliptical pin-fin heat sink, and a cold plate for water cooling. In the chimney, the temperature of flue gases is 450-650K. Although the TEG hot-side temperature and thus the electric power output can be increased by inserting an elliptical pin-fin heat sink into the chimney tunnel to increase the heat transfer area, the pin fin heat sink would cause extra pumping power at the same time. The main purpose of this study is to analyze the effects of geometrical parameters on the electric power output and chimney pressure drop characteristics. The effects of different operating conditions, including various inlet velocities (V_{in}= 1, 3, 5 m/s), inlet temperatures (T_{gas} = 450, 550, 650K) and different fin height (0 to 150 mm) are discussed in detail. The predicted numerical data for the power vs. current (P-I) curve are in good agreement (within 11%) with the experimental data.

***Keywords*—**Thermoelectric generator, Waste heat recovery, Elliptical pin-fin heat sink.

I. Introduction

RECENTLY, applications of thermoelectric technology have been extensively studied due to the increasing emphasis on energy savings and carbon reduction. Thermoelectric generators (TEGs) have potential application for the conversion of low-level thermal energy into electrical power. For waste heat recovery, it is unnecessary to consider the cost of the thermal energy input. In general, a TEG consists of a number of semiconductor pairs that are connected electrically in series and thermally in parallel. Each pair includes a p-type and an n-type element. The working principle of a TEG is based on the Seebeck effect which induces an electromotive force in semiconductor materials due to temperature gradients.

In recent years, there has been growing interest in using various heat sources for TEGs, including combustion waste, geothermal energy, power plants, and other industrial heat generating processes [1], [2]. Thacher, Helenbrook, Karri and Richter [3] investigated the feasibility of waste heat recovery from exhaust in a light truck by connecting a series of 16 TEG modules, and found good performance at high speeds. Champier, Bedecarrats, Rivaletto and Strub [4] investigated the feasibility of using a TEG in an improved biomass fired stove. The maximum power reached by each module varied between 1.7 and 2.3 W, resulting in a temperature difference between the two sides of 433 K. Qiu and Hayden [5] developed a self-powered residential heating system that uses TEG technology. They found the electricity generated was adequate to power all electrical components of a residential central heating system. Hsiao and Chang [6] constructed a mathematic model to predict the performance of a TEG module attached to a waste heat recovery system. The results showed that the TEG module presented better performance on an exhaust pipe as opposed to a radiator.

Since the chimney tunnel is usually made of rectangular pipes, it is feasible to insert a fin heat sink into it to increase the heat transfer area and reduce thermal resistance from the flue gas to the TEG module. However, the disadvantage is that the pressure drop of the system will increase. Behnia, Copeland and Soodphakdee [7] numerically compared the heat transfer performance of various commonly used fin geometries: circular, square, rectangular, and elliptical. They found that elliptical pin-fins outperform than plate-fins. They also found that elliptical fins work best at lower values of pressure drop and pumping work. Li and Chen [8] carried out experiments regarding heat transfer and pressure drop characteristics with circular and elliptical pin fins. They found that the heat transfer performance with elliptical pin fins is better than that with circular pin fins but the flow resistance of the former is much lower than that of the latter. Jang and Tsai [9] numerically optimized TEG module spacing and spreader thickness as used in a waste heat recovery system and solved numerically using the finite difference method along with a simplified conjugate-gradient method. They discussed effects of temperature difference and waste gas heat transfer coefficients, and found that the numerical data were in good agreement with the experimental data. Jang and Tsai [10] investigated the characteristics of heat transfer behavior and power generation of a TEG module with a plate-fin heat sink, both numerically and experimentally. Of note, the optimal fin height H_{fin} was found to be about 50 mm, with a corresponding maximum net power density (P_{net}/A_b) at N = 6,V_{in} = 10 m/s and T_{gas} = 600 K.

The present work focuses on the power generation performance of TEG modules that use elliptical pin-fin as heat sink. The influence of the fin geometrical parameters on the power output and the pressure drop increment is discussed.

J. Y. Jang is with the Department of Mechanical Engineering, National Cheng Kung University, Tainan, Taiwan (Tel.: 886-6-2088573, e-mail: jangjim@mail.ncku.edu.tw).

C. Y Tseng. is with the Department of Mechanical Engineering, National Cheng-Kung University, Tainan, Taiwan (Tel.: 886-6-2757575 ext. 62148, e-mail: n16014140@mail.ncku.edu.tw).

II. Theoretical Model

A schematic diagram of a waste heat recovery system with TEG modules is shown in Fig. 1. Each TEG module is composed of an elliptical pin-fin heat sink, a TEG, and a cold plate based on water cooling. The approximate dimensions of the assembled square TEG unit are 40 mm × 40 mm × 3.3 mm. The TEG converts heat energy into electric power using 49 pairs of p-type and n-type semiconductor legs connected thermally in parallel between the hot waste gas and the cold plate and electrically in series to power the load circuit. The TEG models could be simplified by using the basis of an equivalent current methods, which means an equal electric current and an equal cross area of thermoelectric elements, and thus only one pair of semiconductor elements is considered. In addition, as illustrated in Fig. 2, there are two types of arrangement of the elliptical pin-fin heat sink, namely in-lined and staggered.

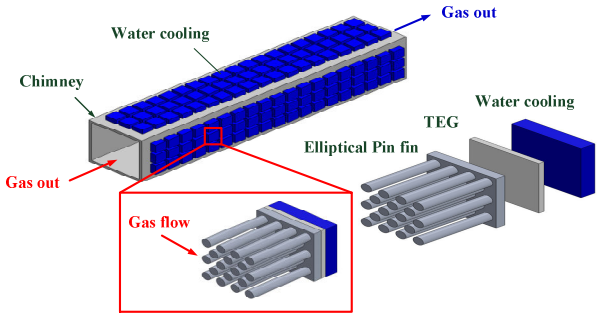

Fig. 1 Schematic diagram of TEG modules with elliptical pin-fin

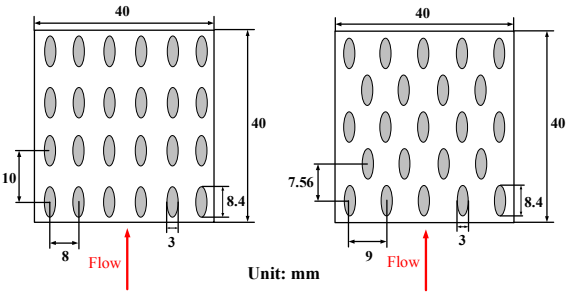

Fig. 2 Arrangement of elliptical pin fins

The three-dimensional heat conduction governing equation under steady state and constant conductivity with no heat generation is:

$$\frac{\partial^2 \mathrm{T}}{\partial x^2}+\frac{\partial^2 \mathrm{T}}{\partial y^2}+\frac{\partial^2 \mathrm{T}}{\partial z^2}=0 \tag{1}$$

The governing equation of the thermal field (T) and electrical potential (V) for the p-type and n-type elements can be expressed as:

$$\mathrm{k}_{P/N}\left(\frac{\partial^2 \mathrm{T}}{\partial x^2}+\frac{\partial^2 \mathrm{T}}{\partial y^2}+\frac{\partial^2 \mathrm{T}}{\partial z^2}\right)+\varepsilon_{P/N}\bar{\mathrm{J}}^2=0 \tag{2}$$

where $k_{P/N}$, $\varepsilon_{P/N}$, and $\alpha_{P/N}$ represent the equivalent thermal conductivity, electrical resistivity, and Seebeck coefficient of the thermoelectric elements, respectively. $\bar{\mathrm{E}}$ and $\bar{\mathrm{J}}$ denote the electrical field and current density, respectively. The governing equation of the electric field under steady state can be written as

$$\bar{\mathrm{E}}=\frac{\partial \mathrm{V}}{\partial x}\bar{i}+\frac{\partial \mathrm{V}}{\partial y}\bar{j}+\frac{\partial \mathrm{V}}{\partial z}\bar{k}\ =-\alpha_{P/N}\left(\frac{\partial \mathrm{T}}{\partial x}\bar{i}+\frac{\partial \mathrm{T}}{\partial y}\bar{j}+\frac{\partial \mathrm{T}}{\partial z}\bar{k}\right)-\varepsilon_{P/N}\bar{\mathrm{J}} \tag{3}$$

The field throughout the conductive regions is calculated based on flux (charge) conservation in each cell. Equation (3) can be rewritten as

$$\frac{\partial^2 \mathrm{V}}{\partial x^2}+\frac{\partial^2 \mathrm{V}}{\partial y^2}+\frac{\partial^2 \mathrm{V}}{\partial z^2}=-\alpha_{P/N}\left(\frac{\partial^2 \mathrm{T}}{\partial x^2}+\frac{\partial^2 \mathrm{T}}{\partial y^2}+\frac{\partial^2 \mathrm{T}}{\partial z^2}\right) \tag{4}$$

For the waste gas flow in the chimney, the fluid is considered incompressible with constant properties and no viscous dissipation. The equations for mass, momentum and energy can be expressed as

$$\frac{\partial \overline{u_i}}{\partial x}=0 \tag{5}$$

$$\rho\frac{\partial}{\partial x_j}\left(\overline{u_j u_i}\right)=-\frac{\partial \overline{P}}{\partial x_i}+\mu\nabla^2\overline{u_i}-\rho\frac{\partial}{\partial x_j}\left(\overline{u_j' u_i'}\right) \tag{6}$$

$$\frac{\partial}{\partial x_j}\rho C_p\left(\overline{u}_j\overline{T}\right)=\overline{u_j}\frac{\partial \overline{P}}{\partial x_j}+\overline{u_j'}\frac{\partial \overline{P'}}{\partial x_j}-\frac{\partial}{\partial x_j}\left(k\frac{\partial \overline{T}}{\partial x_j}-\rho C_p\overline{u_j' T'}\right)-\nabla\cdot\bar{q}_r \tag{7}$$

In the present study, the κ-ε turbulent model was introduced to simulate the flow field more accurately. The κ-ε turbulent equations are:

$$\rho\frac{\partial}{\partial x_j}\left(\overline{u_j}\kappa\right)=\frac{\partial}{\partial x_j}\left[\left(\mu_l+\frac{\mu_t}{\sigma_\kappa}\right)\frac{\partial \kappa}{\partial x_j}\right]+\rho(\mathrm{P_r}-\varepsilon) \tag{8}$$

$$\rho\frac{\partial}{\partial x_j}\left(\overline{u_j}\varepsilon\right)=\frac{\partial}{\partial x_j}\left[\left(\mu_l+\frac{\mu_t}{\sigma_\varepsilon}\right)\frac{\partial \varepsilon}{\partial x_j}\right]+\rho\frac{\varepsilon}{\kappa}(c_1\mathrm{P_r}-c_2\varepsilon) \tag{9}$$

Because the governing equations are elliptical in spatial coordinates, boundary conditions are required for all boundaries of the computational domain. For the gas flow in the chimney, the inlet boundary is assumed to be a uniform velocity distribution, and the ambient pressure is set at the outlet boundary. At the solid-fluid interface, the no-slip condition is specified. For turbulence calculations, the turbulence intensity at the inlet is set to 3 %.

III. Numerical Method

The governing equations and boundary conditions are solved using commercial computational fluid dynamics (CFD)

software. In this study, the governing equations are solved numerically using a control volume base on a finite difference method. Finite difference approximations are employed to discretize the transport equations onto a non-staggered grid mesh system. The computational grid system is shown in Fig. 3. Prior to computation, a thorough verification of the grid-independence of the numerical solution was performed in order to ensure the accuracy and validity of the numerical results. For validating the grid independence, each model was investigated with grid systems that included about 314,873, 406,349, 496,618 and 587,794 nodes, respectively, for the TEG module and the chimney waste gas with built-in fins. It was found that the relative errors of the chimney pressure drop between the solutions obtained with 496,618 and 587,794 nodes are less than 1.23%. When the results satisfy the following conditions, the solutions are treated as being converged:

$$R_{\varphi} = \left| \frac{\phi_{i+1} - \phi_i}{\phi_i} \right| \tag{10}$$

$$\sum R_{\phi} < 10^{-5} \quad , \quad \phi = u, v, w, \kappa, \varepsilon, p, T, V \tag{11}$$

where R is the residual sum and ϕ is the general dependent variables. The subscript i indicates the number of iterations.

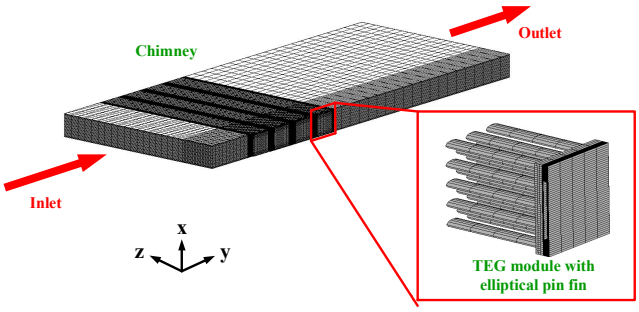

Fig. 3 Computational grid system

IV. Experimental Setup

Numerical predictions of the module performance obtained from the CFD code were verified with experimental results. As illustrated in Fig. 4, the experimental setup mainly composed of three parts which are a wind tunnel system, water circulating system and an electrical network.

The wind tunnel system consists of a blower, 12 annular heating units assembled on a round stainless duct, a flow settling chamber, the test section, and an exhaust pipe. The air flow was driven by a 5 HP centrifugal fan with a variable-frequency converter to provide various inlet velocities for air to flow along the wind tunnel and pass through the TEG module to simulate the flow in the chimney. The air velocity in the test section was measured by a hot wire with 2.0% accuracy. The heating section of the experimental setup used 12 heaters that could supply a maximum heat load of about 35 kW. In addition, the TEG module was built-in from the top surface of the test section. Thermal grease was used to minimize the thermal contact resistance between the TEG and the plate-fin, which was made of aluminum (Al 6063) without additional surface treatment. Moreover, the air temperatures at the inlet and the exit zones across the test section were measured by two pre-calibrated RTDs (pt-100Ω) with accuracy within ±0.05 K. To reduce heat loss, the wind tunnel system was surrounded by an insulator.

The TEG module was cooled by water pumped in a closed circulating system that includes a flow meter and a thermostat reservoir with a temperature-controlled immersion heater to maintain the water at 27°C. The water volumetric flow rate was measured by a magnetic volume flow meter with 0.002 L/s resolution. T-type thermal couples were embedded in the inlet and outlet of the cooling water system to record temperature during measurements.

In the electric network, a high-power electrical resistor array was connected in series to the TEG module to capture the matching load for the maximum power output. An ammeter was connected in series to measure the current in the circuit and a voltmeter was connected in parallel to measure the voltage cross the external load resistor. A digital multi-meter (Fluke 170) was used to measure the voltage with an accuracy of 0.15% and the current with an accuracy of 1.0%. All the data signals were collected and converted using a data acquisition system (a hybrid recorder).

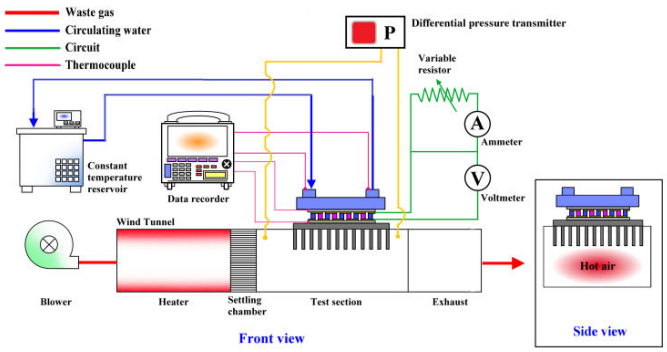

Fig. 4 Schematic diagram of experimental setup

V. Results and Discussion

Figs. 5 and 6 show the temperature and electric potential distributions of the TEG module with an elliptical pin-fin heat sink in in-lined and staggered arrangements, respectively, for a fin height H_f of 50 mm and total heat transfer area are approximately 225cm^2 for both arrangements. The inlet velocity in the chimney V_{in} was 3 m/s, and the inlet temperature T_{gas} was 550K. It is seen that the hot-side temperature (T_h) of the TEG module with a staggered pin-fin heat sink is higher than that of the module with an in-lined arrangement. The staggered pin-in heat sink increases the TEG hot-side temperature, and thus the staggered pin-fin heat sink has better heat transfer performance. The open-circuit voltages V_{oc} are 1.215 and 1.175 V for TEG modules with staggered and in-lined pin-fin arrangements, respectively.

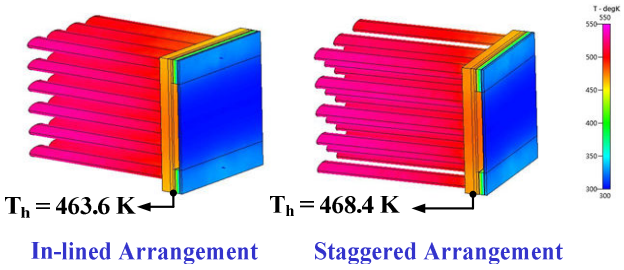

Fig. 5 Temperature distributions of TEG module

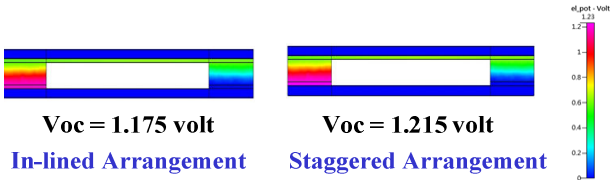

Fig. 6 Electric potential distributions of TEG

Figs. 7 and 8 show the voltage-current (V-I) and the power-current (P-I) curves of the TEG module with in-lined and staggered pin fin arrangements, respectively, for various inlet velocities (V_{in}= 1, 3, 5 m/s) and waste gas temperature T_{gas} = 450K and with fin height 50mm. The experimental results are denoted by circles. It can be seen that the predicted numerical data for the P-I curves are in good agreement (within 11%) with the experimental data. It can also be found that the maximum power, P_{max}, occurs when the external load resistance is to equal the effective internal resistance of the TEG.

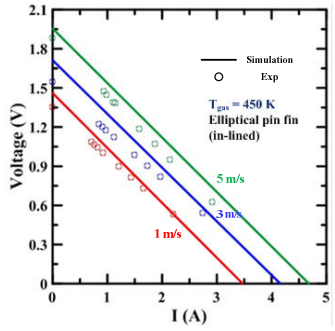

(a) V-I curve

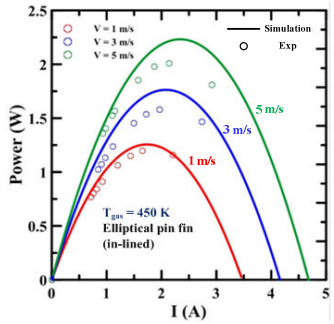

(b) P-I curve

Fig. 7 V-I and P-I curves for with in-lined arrangement

In order to evaluate the heat transfer performance and pressure drop in a tunnel of the elliptical pin fin, a comparison was made between a conventional plate-fin [10] and an elliptical pin-fin. Fig. 9 shows the variation of the pumping power per unit area with elliptical and plate fin geometries for various inlet gas velocities and with fin height 50mm. The elliptical pin-fin heat sink produces a higher pressure drop than that by the conventional plate-fin heat sink, and the pressure drop of a staggered elliptical pin fin is slightly higher than that of an in-lined elliptical pin-fin. The pumping power values for plate-fin, in-lined elliptical pin fin, and staggered elliptical pin fin are 0.0448, 0.088 and 0.0976 W for an inlet velocity of 5m/s.

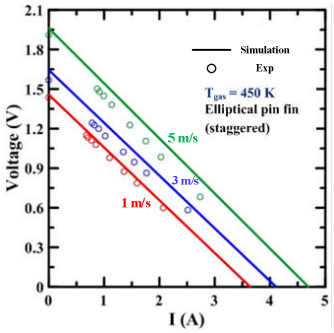

(a) V-I curve

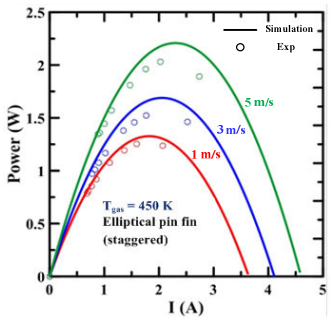

(b) P-I curve

Fig. 8 V-I and P-I curves with staggered arrangement

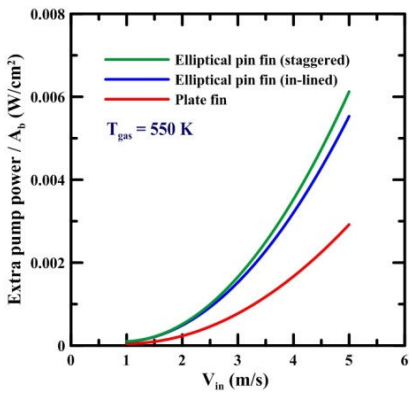

Fig. 9 $P_{pump\ power}$/A vs. velocity for various fin geometries

Figs. 10 and 11 show the variations of P_{ideal}/A (ideal electrical power density) and P_{net}/A (net electrical power density) for gas inlet temperature of 550K and 650K,

respectively, with inlet velocity (V_{in} = 1-5 m/s) and with height 50mm for the plate-fin, in-lined elliptical pin-fin, and staggered elliptical pin-fin. The three types of heat sinks fin are also compared using the same heat transfer area. The electrical power output is increased with increasing inlet temperature or inlet velocity. Although the elliptical pin-fin heat sink has better heat transfer performance than that of the plate-fin heat sink, its pressure drop is higher. There is a trade-off between heat transfer performance and extra pumping power. In order to know the net electric power that the TEG module could actually generate, P_{ideal} should minus the extra pumping power to obtain the actual power that could be used in other purpose without any cost uncounted. The net power density is denoted by solid line, and the ideal power density is denoted by dashed line. The TEG module with an elliptical pin-fin heat sink has higher ideal power density than that obtaining using a plate-fin. For a gas inlet temperature of 550K and a gas inlet velocity of 5 m/s, the P_{net}/A values of TEG modules with a staggered elliptical pin fin, in-lined elliptical pin fin, and plate-fin are 0.231, 0.2195, and 0.1821 W/cm^2, respectively. The TEG module with a staggered pin fin has the best power generation performance. For an inlet velocity of 5m/s and an inlet temperature of 650K, the P_{net}/A values of TEG modules with a plate-fin, in-lined elliptical pin fin, and staggered elliptical pin fin are 0.287, 0.362, and 0.375 W/cm^2, respectively. The elliptical pin fin can improve P_{net}/A by about 1.26-1.31 times compared to that for a plate-fin.

Figs. 12 and 13 show the variations in the pump power density and the electrical power density vs. different fin height, respectively, for three gas inlet velocities (V_{in}= 1, 3, and 5m/s) at T_{gas} = 550K. As expected, the pump power is increased with increasing fin height (H_{fin}) or gas inlet velocity (V_{in}). When the fin height of the staggered pin-fin heat sink was increased from 0 to 150 mm, the heat transfer area increased from 16 to 418.1 cm^2. Thus, the power density is increased. When the gas velocity is low, the ideal power density and the net power density do not obviously diverge with increasing in the fin height. However, they obviously diverge when the gas inlet velocity is high. Thus, there is a proper fin height (H_{fin}) exists in correspondence with the optimal net electrical power density.

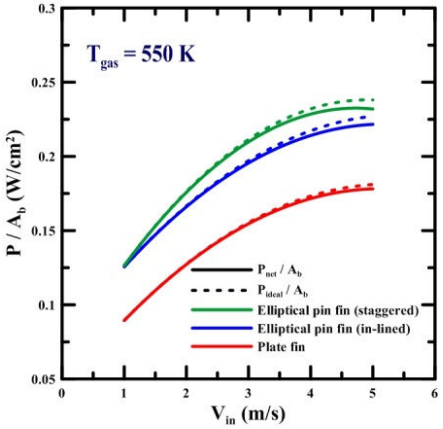

Fig. 10 P_{net}/A and P_{ideal}/A vs. velocity for various fin geometries

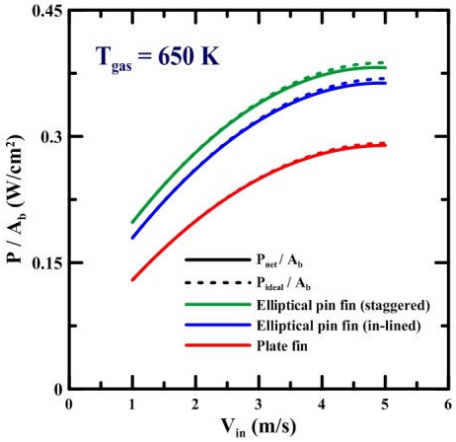

Fig. 11 P_{net}/A and P_{ideal}/A vs. velocity for various fin geometries

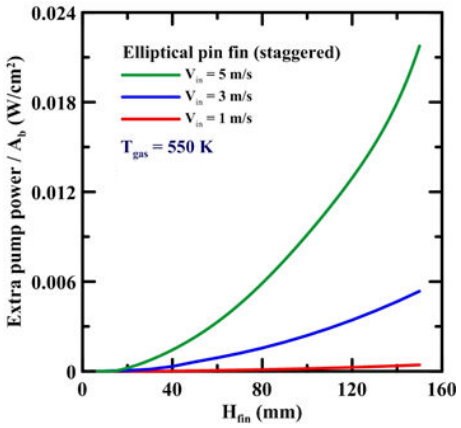

Fig. 12 $P_{pump\ power}/A$ vs. fin height for various gas velocities

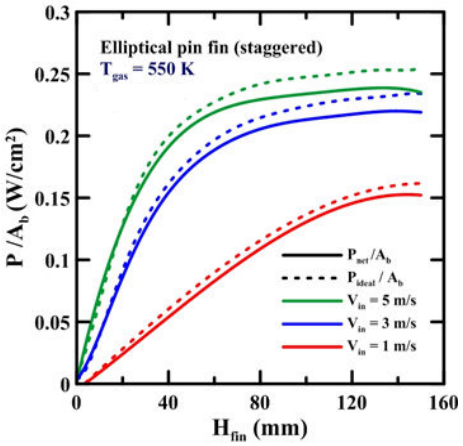

Fig. 13 P_{net}/A and P_{ideal}/A vs. fin height for various gas velocities

VI. Conclusion

In the present study, a TEG module with an elliptical pin-fin heat sink for waste heat recovery was investigated numerically and experimentally. To evaluate the extra pressure drop, ideal electrical power density, and net electrical power density, which are the key parameters, the governing equations were solved using the finite difference method. The following

conclusions were obtained:

1. The predicted numerical data for the P-I curves are in good agreement (within 11%) with the experimental data.
2. The elliptical pin-fin heat sink produces a higher pressure drop than that obtained with the conventional plate-fin heat sink, and the pressure drop of the staggered elliptical pin fin is slightly higher than that of the in-lined elliptical pin-fin.
3. For an inlet velocity of 5m/s and an inlet temperature of 650K, the net electrical power density of TEG modules with a plate-fin, in-lined elliptical pin fin, and staggered elliptical pin fin are 0.287, 0.362, and 0.375 W/cm2, respectively. The elliptical pin fin can improve the electrical power density by about 1.26-1.31 times compared to that for a conventional plate-fin.
4. There is a proper fin height (H_{fin}) exists in correspondence with the optimal net electrical power density.

ACKNOWLEDGEMENT

The financial support by the ministry of science and technology, Taiwan, ROC, under grant MOST 103-2221-E-006 -130 is highly appreciated.

NOMENCLATURE

A_{fin}	fin surface area
A_{TEG}	TEG surface area
$\bar{E}$	electric field
h_c	cooling water heat transfer coefficient
I	electric current
$\bar{J}$	current density
$k_{P/N}$	equivalent thermal conductivity of TEG
H_{fin}	fin height
N	number of fin
P	electric power output
P	pressure
P_{ideal}	electric power output before counting pumping power
P_{max}	maximum electric power output
P_{net}	net electric power
P_r	turbulent kinetic energy production rate
T	temperature
T_h	hot side temperature of TEG
T_{gas}	Temperature of waste gas
V	electric potential
V_{oc}	open circuit electric potential
V_{in}	waste gas inlet velocity
X_t	Transverse fin pitch
u_i	velocity component
$\alpha_{P/N}$	equivalent Seebeck coefficient of TEG
ΔP	chimney tunnel pressure drop
ΔT	temperature difference between the waste-gas and the cooling water
ε	turbulent energy dissipation ratio
$\varepsilon_{P/N}$	equivalent electrical resistivity of TEG
κ	turbulent kinetic energy
μ	dynamic viscosity
μ_l	laminar viscosity
μ_t	turbulent viscosity
ρ	gas density
σ_ε	Prandtl number for turbulent kinetic energy
σ_κ	Prandtl number for turbulent energy dissipation

REFERENCES

[1] K. Ono, R. O. Suzuki, "Thermoelectric power generation: Converting low-grade heat into electricity," *JOM*, Vol. 50, pp.49-51, 1998.

[2] D. M. Rowe, "Thermoelectrics, an environmentally-friendly source of electrical power," *Renewable energy*, Vol 16, pp.1251-1256, 1999.

[3] E. F. Thacher, B. T. Helenbrook, K. A. Karri, C. J. Richter, "Testing of an automobile exhaust thermoelectric generator in a light truck," *Proceedings of the Institution of Mechanical Engineers - Part D: Journal of Automobile Engineering*, Vol. 221, pp. 95-107, 2007.

[4] D. Champier, A. Bedecarrats, B. Rivaletto, H. Strub. "Thermoelectric power generation from biomass cook stoves," *Energy*, Vol.35, pp.935-942, 2010.

[5] K. Qiu, A. C. S. Hayden, "Development of a Thermoelectric Self-Powered Residential Heating System," *Journal of Power Sources*, Vol. 180, pp. 884-889, 2008.

[6] Y. Y. Hsiao, W. C. Chang, S. L. Chen, "A Mathematic Model of Thermoelectric Module with Applications on Waste Heat Recovery from Automobile Engine," *Energy*, Vol. 35, pp. 1447-1454, 2010.

[7] M. Behnia, D. Copeland, D. Soodphakdee, "A Comparison of Heat Sink Geometries for Laminar Forced Convection: Numerical Simulation of Periodically Developed Flow," *Thermal and Thermomechanical Phenomena in Electronic Systems, 1998. ITHERM '98. The Sixth Intersociety Conference on*, pp. 310-315, 1998.

[8] Q. L. Li, Z. Chen, "Heat transfer and pressure drop characteristics in rectangular channels with elliptic pin fins," *International Journal of Heat and Fluid Flow*, Vol. 19, Issue 3, pp. 245-250, 1998.

[9] J. Y. Jang, Y. C. Tsai, "Optimization of Thermoelectric Generator Module Spacing and Spreader Thickness Used in a Waste Heat Recovery System," *Applied Thermal Engineering*, Vol. 51, pp. 677-689, 2013.

[10] J. Y. Jang, Y. C. Tsai, C. W. Wu, "A Study of 3-D Numerical Simulation and Comparison with Experimental Results on Turbulent Flow of Venting Flue Gas Using Thermoelectric Generator Modules and Plate Fin Heat Sink," *Energy*, Vol. 53, pp 270-281, 2013.

Jiin-Yuh Jang is a Distinguished Professor in the Department of Mechanical Engineering at National Cheng Kung University, Tainan, Taiwan. He received his Ph.D. in mechanical engineering from the State University of New York at Buffalo, USA, in 1983. His research interests include heat exchanger CAD design, numerical and experimental studies of heat exchangers, energy conversion, and air conditioning. He is an ASHRAE and ASME fellow.

Chia-Yu Tseng is a M.S. graduate student (2014) in the Department of Mechanical Engineering, National Cheng-Kung University, Tainan, Taiwan. He received his B.S. degree from the Department of Engineering Science, National Cheng-Kung University, Tainan, Taiwan, in 2012.